BMJ Open Diabetes Research & Care

# Differential DNA methylation profile in infants born small-for-gestational-age: association with markers of adiposity and insulin resistance from birth to age 24 months

Marta Diaz,[1,2] Edurne Garde,[1,2] Abel Lopez-Bermejo,[3] Francis de Zegher,[4] Lourdes Ibañez [1,2]

**To cite:** Diaz M, Garde E, Lopez-Bermejo A, *et al*. Differential DNA methylation profile in infants born small-for-gestational-age: association with markers of adiposity and insulin resistance from birth to age 24 months. *BMJ Open Diab Res Care* 2020;**8**:e001402. doi:10.1136/bmjdrc-2020-001402

► Supplemental material is published online only. To view please visit the journal online (http://dx.doi.org/10.1136/bmjdrc-2020-001402).

Received 24 March 2020
Revised 4 July 2020
Accepted 25 August 2020



For numbered affiliations see end of article.

**Correspondence to**
Dr Lourdes Ibañez;
libanez@hsjdbcn.org

## ABSTRACT

**Introduction** Prenatal growth restraint followed by rapid postnatal weight gain increases lifelong diabetes risk. Epigenetic dysregulation in critical windows could exert long-term effects on metabolism and confer such risk.

**Research design and methods** We conducted a genome-wide DNA methylation profiling in peripheral blood from infants born appropriate-for-gestational-age (AGA, n=30) or small-for-gestational-age (SGA, n=21, with postnatal catch-up) at age 12 months, to identify new genes that may predispose to metabolic dysfunction. Candidate genes were validated by bisulfite pyrosequencing in the entire cohort. All infants were followed since birth; cord blood methylation profiling was previously reported. Endocrine-metabolic variables and body composition (dual-energy X-ray absorptiometry) were assessed at birth and at 12 and 24 months.

**Results** *GPR120* (*cg14582356*, *cg01272400*, *cg23654127*, *cg03629447*), *NKX6.1* (*cg22598426*, *cg07688460*, *cg17444738*, *cg12076463*, *cg10457539*), *CPT1A* (*cg14073497, cg00941258, cg12778395*) and *IGFBP 4* (*cg15471812*) genes were hypermethylated (*GPR120*, *NKX6.1* were also hypermethylated in cord blood), whereas *CHGA* (*cg13332653*, *cg15480367*, *cg05700406*), *FABP5* (*cg00696973*, *cg10563714*, *cg16128701*), *CTRP1* (*cg19231170*, *cg19472078*, *cg0164309*, *cg07162665*, *cg17758081*, *cg18996910*, *cg06709009*), *GAS6* (*N/A*), *ONECUT1* (*cg14217069*, *cg02061705*, *cg26158897*, *cg06657050*, *cg15446043*) and *SLC2A8* (*cg20758474*, *cg19021975*, *cg11312566*, *cg12281690*, *cg04016166*, *cg03804985*) genes were hypomethylated in SGA infants. These genes were related to β-cell development and function, inflammation, and glucose and lipid metabolism and associated with body mass index, body composition, and markers of insulin resistance at 12 and 24 months.

**Conclusion** In conclusion, at 12 months, abnormal methylation of *GPR120* and *NKX6.1* persists and new epigenetic marks further involved in adipogenesis and energy homeostasis arise in SGA infants. These abnormalities may contribute to metabolic dysfunction and diabetes risk later in life.

## Significance of this study

### What is already known about this subject?

- There is increasing evidence concerning the fetal programming of adult pathologies, including obesity, diabetes and cardiovascular disease. It is recognized that an adverse intrauterine environment resulting in small-for-gestational-age (SGA) fetuses can induce changes in the epigenome to allow fetal adaptation. In addition, SGA infants who experience a rapid postnatal catch-up in weight are at increased risk for diabetes later in life. Thus, although the sequence of events is not well understood, the prenatal as well as the postnatal environment may ultimately induce changes in DNA methylation that lead to metabolic dysfunction through modulation of the expression levels of key genes directly or indirectly involved in the control of metabolic processes.

### What are the new findings?

- SGA infants show a differential DNA methylation profile in peripheral blood at age 12 months as compared with appropriate-for-gestational-age infants (AGA); some of the altered epigenetic marks were already present at birth (in both the *GPR120* and *NKX6.1* genes) whereas others appear at the age of 12 months.
- Dysmethylated genes relate to β-cell biology, regulation of glucose and lipid metabolism and inflammation, and associated with body mass index, body composition parameters and markers of insulin resistance at 12 and 24 months.
- Dysfunction of dysmethylated genes may induce long-term changes in gene expression contributing to the genesis of metabolic disturbances, which in turn may increase the future risk for diabetes of SGA infants.

## INTRODUCTION

Low birth weight followed by rapid postnatal weight gain has been associated with increased metabolic risk in adulthood

## Significance of this study

### How might these results change the focus of research or clinical practice?

- The degree of abnormal methylation of the reported genes may become a novel biomarker for the early identification of those SGA infants at high risk for developing metabolic disorders later in life. Follow-up of these infants with personalized lifestyle measures will possibly prevent a rapid catch-up in body weight that, besides the genetic and epigenetic background, seems to be a key driver for the development of insulin resistance and diabetes.

including for obesity, type 2 diabetes and cardiovascular disorders.[1 2] The extent of this mismatch between the prenatal and postnatal environments—as judged by the Z-score change from weight at birth to body mass index (BMI) in childhood—appears to be critical in metabolic programming, as it relates closely to central (hepatovisceral fat) and insulin resistance.[3 4] Along these lines, catch-up infants born small-for-gestational-age (SGA, birth weight below −2 SD), and particularly those who receive enriched formulas and have a faster weight gain, depict low levels of high molecular weight (HMW) adiponectin and are less insulin sensitive and more abdominally adipose than those born appropriate-for-gestational-age (AGA).[5] Although the mechanisms underlying this sequence of events have not been elucidated in full, there is increasing evidence of the key role played by epigenetics—especially DNA methylation—in the fetal programming of adult pathologies.[6–8] DNA methylation is modulated by environmental factors, particularly by nutrition, and it has been proved that an adverse nutritional environment during the perinatal period can lead to persistent epigenetic modifications producing stable changes in gene expression later in life.[9–11] Methylation of cytosine bases in CpG dinucleotides induces chromatin modifications leading to repression of gene expression by recruitment of methyl-binding and chromatin remodeling proteins, or by blocking transcriptional machinery from accessing start sites on a gene's promoter.[12] We have recently reported a differential methylation and expression pattern of genes involved in the regulation of glucose and lipid metabolism in placenta and cord blood of SGA infants, which may influence fetal growth, early adipogenesis and later diabetes risk.[13] Remarkably, DNA methylation levels have been shown to change more rapidly in the immediate postnatal years, tending to stabilize beyond age 7.[14] However, reports on DNA methylation patterns during early childhood are scarce, and none has assessed simultaneously endocrine-metabolic parameters and/or body composition.[15–17] Here, we tested whether differential DNA methylation patterns persist in catch-up SGA infants—as compared with AGA infants—and whether new epigenetic marks involved in the control of energy metabolism arise by age 12 months. We also assessed the associations among those differentially methylated genes and endocrine-metabolic and body composition variables at age 12 and 24 months.

## RESEARCH DESIGN AND METHODS

### Study population

The study cohort consisted of 51 infants born either AGA (n=30; 57% female) or SGA (n=21; 57% female) who participated in a previous study assessing DNA methylation in placenta and cord blood of SGA versus AGA infants and its association with endocrine-metabolic parameters and body composition,[13] and who were subsequently followed up to age 24 months.

The specific inclusion criteria were (1) singleton pregnancy, absence of maternal pathology (hypertension, preeclampsia or gestational diabetes) and drug addiction; (2) term birth (37–42 weeks) with a birth weight range between −1.1 and +1.1 SD (AGA) and below −2 SD (SGA); (3) spontaneous catch-up in weight and length, defined as weight and length Z-score >−2.0 by age 12 months[18]; (4) auxological (weight, length, BMI and BMI Z-score), endocrine-metabolic assessments and body composition at birth, and at 12 and 24 months (see below); and (5) written, informed consent in Spanish/Catalan language. Exclusion criteria were congenital malformations or complications at birth (need for resuscitation or parenteral nutrition). Eighty-six per cent of AGA infants were exclusively breast fed from 0 to 4 months, versus 59% of SGA infants.

### Assessments

Infant's weight and length were measured at birth and at age 15 days, as reported,[13] and again at 12 and 24 months. BMI was calculated at each time point, and BMI Z-scores were derived from country-specific and sex-specific references.[19]

Blood samples were obtained at birth from the umbilical cord (before placental separation)[13] and in the morning state after an overnight fast at age 12 and 24 months. Whole blood collected in EDTA tubes was used for DNA extraction at age 12 months. Serum samples were also obtained at 12 and at 24 months and kept at −80°C.

The entire cohort (n=51) completed the first year of follow-up including auxological, endocrine-metabolic and body composition assessments. In the subsequent year, n=7 patients dropped out from the study, so that completion of all assessments could only be performed in n=44 infants at age 24 months (26 AGA and 18 SGA) (online supplemental figure 1, flow chart). The characteristics of the patients lost to follow-up did not differ from those who completed the study (data not shown).

Serum glucose was measured by the glucose oxidase method. Insulin, IGF-I and lipids were assessed by immunochemiluminiscence (DPC IMMULITE 2500; Siemens, Erlangen, Germany); intra-assay and inter-assay coefficients of variation were <10%. Insulin resistance was estimated with the homeostatic model assessment (fasting

insulin (mU/L)×fasting glucose (mmol/L)/22.5). HMW adiponectin was assessed by ELISA (R&D Systems, Minneapolis, MN, USA); intra-assay and inter-assay coefficients of variation were <9%.

Body composition was assessed at age 15 days and at 12 and 24 months, by dual X-ray absorptiometry with a Lunar Prodigy coupled to Lunar software (Lunar, Madison, WI, USA), adapted for infants. CVs were <3% for fat and lean mass.

### DNA extraction and bisulfite conversion

DNA was extracted from peripheral blood samples by the phenol–chloroform method (Promega, Madison, WI, USA), following the manufacturer's protocol. DNA quality and concentration were assessed using a UV–VIS spectrophotometer (Nanodrop 1000; Agilent Technologies, Wilmington, DE, USA). To minimize batch effect, samples were randomized per birth weight and sex. Bisulfite (BS) conversion of 300 ng DNA was performed using the Methylcode Bisulfite Conversion Kit (Invitrogen, Carlsbad, CA, USA) following manufacturer's guidelines. Conversion quality control was conducted by quantitative PCR (qPCR) and melting curve analysis.

### DNA methylation microarray in peripheral blood samples

DNA methylation profiling at age 12 months was performed in eight AGA and eight SGA samples with the Agilent DNA Methylation array (ID 049738; Agilent Technologies), which examines 27,800 highly informative CpG sites located within the proximal promoter regions of 14,475 genes. Nearly 100% of these CpG sites were localized within CpG islands. The process for isolating methylated DNA from purified DNA samples, and labeling and hybridization to Human DNA Methylation Array, was conducted following the manufacturer's protocol (Agilent Microarray Analysis of Methylated DNA Immunoprecipitation V.1.1; Agilent Technologies), as previously described.[13]

### Pre-processing and analysis of Agilent DNA methylation microarray

Microarray image was scanned using Agilent SureScan and raw β values were exported using Agilent's Feature Extraction Software (V.10.7). Raw methylation data were preprocessed using *Agilent Genomic Workbench v6.5* BATMAN algorithm (Bayesian Tool for Methylation Analysis) and normalized to control probes present on the array. Outlier features on the arrays were flagged by the same software package. Values were $\log_2$-transformed and logged data were used for principal component analysis (PCA) and for statistical analysis. The Welch T-test was used for identification of differentially methylated genes. An individual probe was considered differentially methylated if its p value was <0.05 (not corrected for multiple testing) and if the effect size (Cohen's d) of t-tests was ≥0.25 (range 0.25–0.8). The resulting p values for each gene were then adjusted for multiple testing using the Benjamini-Hochberg method with a false discovery rate threshold of 10%.

### GO enrichment and KEGG pathway analysis

The identified differentially methylated CpGs between AGA and SGA subgroups were assigned to linked genes using the Agilent DNA methylation microarray annotation file. To investigate the biological relevance of these genes, we performed a Gene Ontology (GO) analysis (http://www.geneontology.org). Significantly enriched (p<0.01) GO terms in SGA versus AGA infants were obtained and subdivided into three categories "Biological Processes", "Molecular functions" and "Cellular components". Gene networks and canonical pathways representing key genes were identified using the KEGG (Kyoto Encyclopedia of Genes and Genomes) software.

### Selection of candidate genes for validation by bisulfite pyrosequencing

Genes showing a differential DNA methylation pattern between the AGA and SGA subgroups were ranked according to their significance level, and those with the lowest adjusted p value ($\leq 10^{-3}$) that were related to energy metabolism were validated in the entire population (30 AGA, 21 SGA) by pyrosequencing. Candidate genes were *GPR120* (G protein–coupled receptor 120), *NKX6.1* (NKX6 homeodomain 1), *IGFBP4* (Insulin-like growth factor binding protein 4), *FABP5* (Fatty acid binding protein 5), *CTRP1* (Complement C1q tumor necrosis factor–related protein 1), *GAS6* (Growth arrest specific 6), *ONECUT1* (One cut homeobox 1), *CHGA* (Chromogranin A), *SLC2A8* (Solute carrier family 2 member 8), *CPT1A* (Carnitine palmitoyltransferase 1A), *SIK2* (Salt inducible kinase 2) and *TRAF2* (TNF receptor associated factor 2).

### Amplification of differentially methylated genes and bisulfite pyrosequencing

Specific pyrosequencing primers and pre-designed PCR primers flanking all CpG islands from promoter regions of the selected genes were used for validation: *GPR120* (PM00044758), chromosome 10, bp 95325316–95327446 (4 CpG sites); *NKX6.1* (PM00019299), chr 4, bp 85417332–85419573 (5 CpG sites); *IGFBP4* (PM00181258), chr 17, bp 38599248–38601371 (4 CpG sites); *FABP5* (PM00036694), chr 8, bp 82192382–82194533 (5 CpG sites); *CTRP1* (PM00182245), chr 17, bp 77019096–77021302 (7 CpG sites); *GAS6* (PM00055216), chr 13, bp 114534252–114536397 (4 CpG sites); *ONECUT1* (PM00059976), chr 15, bp 53082181–53084445 (5 CpG sites); *CHGA* (PM00056070), chr 14, bp 93388198–93390313 (4 CpG sites); *SLC2A8* (PM00142065), chr 9, bp 130158218–130160383 (6 CpG sites); *CPT1A* (PM00152285), chr 11, bp 68610165–68612396 (6 CpG sites); *SIK2* (PM00154672), chr 11, bp 111471855–111473975 (6 CpG sites); *TRAF2* (PM00141302), chr 9, bp 139779587–139781726 (5 CpG sites).

Bisulfite-converted DNA (1 µL) was used as template for each qPCR in a final volume of 25 µL. Hot-start PCR was performed using the PyroMark PCR kit (Qiagen, Germantown, USA) and the correct size of the PCR product was verified by gel electrophoresis. PCR amplicons were purified and analyzed using the PyroMark Q96 ID system and evaluated using the PyroMark software V.2.5 (Qiagen). The methylation level of each CpG site was estimated by the proportion of C (%) in each region. The methylation status of each gene was assessed as the percentage of average methylation at targeted CpG sites.

### Statistics and ethics

Statistical analyses were performed using SPSS software V.23.0. Unpaired t-test was used to study differences between AGA and SGA subgroups. Correlation and stepwise multiple regression analysis were used to study the associations between methylation status at age 12 months, and auxological, endocrine-metabolic and body composition parameters. Covariance analysis was used to adjust for sex and BMI Z-score. The level of significance was set at $p < 0.05$.

The study was approved by the Institutional Review Board of Hospital Sant Joan de Déu at Barcelona University; written informed consent was obtained before delivery.

## RESULTS

### Clinical, endocrine-metabolic and body composition variables

Table 1 summarizes the main clinical, endocrine-metabolic and body composition variables of the studied population. At birth, SGA infants displayed lower circulating levels of IGF-I, and less fat, lean mass and abdominal fat, as reported.[13] At age 12 months, SGA infants normalized their circulating IGF-I levels, as well as their lean mass and abdominal fat, although they remained lighter.[5] The pattern was similar at age 24 months.

### DNA methylation patterns in SGA versus AGA infants

We identified a total of 129 genes differentially methylated in SGA versus AGA infants at age 12 months. Among those, 51 were hypermethylated and 78 were hypomethylated (online supplemental tables 1–4). There were no differences in methylation profile according to early nutrition (breast vs formula feeding 0–4 months), and thus the results within each the AGA and SGA subgroups were pooled for analysis.

The PCA score plot showed a clear separation between the AGA and SGA subgroups, with distinct DNA methylation profiles aggregating together within the same group (figure 1). The three principal components explained 86.3% of the variance observed between subgroups.

### GO functional analysis and KEGG enrichment analysis

To explore potential molecular mechanisms related to birth weight, differentially methylated genes (DMG) were analyzed using GO functional analysis and KEGG enrichment analysis. The enrichment analyses of GO are summarized in table 2. A total of 84 biological processes, 55 molecular functions and 17 cellular components were enriched among the DMG. Regarding biological processes and molecular function, regulation of metabolic processes and organ development together with DNA binding and transcription regulation were the most enriched terms in the respective categories.

The top 10 KEGG pathways of the DMG were enriched in lipid and glucose metabolism, cell development and function, cellular signaling, DNA binding, transcription regulation, regulation of immunity, neural differentiation, and regulation of apoptosis and potassium channel (table 3).

### Validation of methylation status by pyrosequencing in SGA versus AGA infants

Bisulfite pyrosequencing confirmed that 10 of the 12 candidate genes were differentially methylated in SGA versus AGA infants; specifically, *GPR120* (*cg14582356*, *cg01272400*, *cg23654127*, *cg03629447*), *NKX6.1* (*cg22598426*, *cg07688460*, *cg17444738*, *cg12076463*, *cg10457539*), *CPT1A* (*cg14073497*, *cg00941258*, *cg12778395*) and *IGFBP4* (*cg15471812*) were hypermethylated (all $p<0.0001$), whereas *CHGA* (*cg13332653*, *cg15480367*, *cg05700406*), *FABP5* (*cg00696973*, *cg10563714*, *cg16128701*), *CTRP1* (*cg19231170*, *cg19472078*, *cg0164309*, *cg07162665*, *cg17758081*, *cg18996910*, *cg06709009*); *GAS6* (*N/A*), *ONECUT1* (*cg14217069*, *cg02061705*, *cg26158897*, *cg06657050*, *cg15446043*) and *SLC2A8* (*cg20758474*, *cg19021975*, *cg11312566*, *cg12281690*, *cg04016166*, *cg03804985*) were hypomethylated ($p=0.002$ for *FABP5*; $p<0.0001$ for the other five genes) in SGA infants (figure 2). These differences were maintained after adjusting for sex and BMI Z-score. Pyrosequencing did not confirm a differential methylation pattern in *SIK2* and *TRAF2*.

### Correlation analyses

Bivariate correlations between gene methylation levels at age 12 months and selected clinical, endocrine-metabolic and body composition parameters are summarized in online supplemental table 5.

Hypermethylation of *GPR120*, *NKX6.1* and *CPT1A*, as well as hypomethylation of *CHGA*, *CTRP1*, *GAS6*, *ONECUT1* and *SLC2A8* associated with lower BMI Z-scores, and with less fat and lean mass at age 12 months.

At age 24 months, methylation status of *GPR120*, *NKX6.1*, *CTRP1* and *CPT1A* still associated with lower fat and lean mass whereas *SLC2A8* was positively correlated with lean mass. The methylation pattern of all these genes (except for *CPT1A*) together with *ONECUT1* associated with lower BMI Z-score at 24 months. The changes in fat mass between 0–12 and 0–24 months showed a negative correlation with *GPR120* and *NKX6.1* methylation levels.

The methylation profile of *GPR120*, *NKX6.1*, *CHGA*, *GAS6*, *ONECUT1*, *SLC2A8* and *FABP5* associated positively with HOMA-IR at 12 and 24 months, and with 0–12 month and 0–24 month changes in HOMA-IR and IGF-I levels. Hypermethylation of *IGFBP4* directly associated with IGF-I levels at 12 and at 24 months and with IGF-I changes between 0 and 24 months.

**Table 1** Clinical, endocrine-metabolic and imaging data from infants born appropiate-for-gestational-age (AGA, N=30) or small-for-gestational-age (SGA, N=21)

| | Baseline | | 12 months | | Δ0–12 months | | 24 months | | Δ0–24 months | |
|---|---|---|---|---|---|---|---|---|---|---|
| **Anthropometry** | **AGA 30** | **SGA 21** | **AGA** | **SGA** | **AGA** | **SGA** | **AGA** | **SGA** | **AGA** | **SGA** |
| Sex (% female) | 56.70% | 57.10% | – | – | – | – | – | – | – | – |
| Gestational age (weeks) | 40.2±0.2 | 38.7±0.3† | – | – | – | – | – | – | – | – |
| Weight Z-score | 0.1±0.1 | −2.3±0.1† | −0.1±0.3 | −1.5±0.2† | −0.2±0.3 | **0.8±0.2*** | 0.0±0.3 | −1.4±0.3† | −0.1±0.3 | **0.9±0.3*** |
| BMI Z-score | 0.5±0.1 | −1.3±0.2† | −0.1±0.3 | −1.2±0.3‡ | −0.6±0.3 | 0.1±0.4 | 1.3±0.8 | −0.1±0.8 | −0.8±0.3 | 1.2±0.3 |
| Placental weight (kg) | 0.6±0.02 | **0.5±0.03*** | – | – | – | – | – | – | – | – |
| Endocrine-metabolic variables | | | | | | | | | | |
| HOMA-IR | 1.2±0.3 | 1.0±0.3 | 0.7±0.2 | 0.9±0.3 | −0.5±0.4 | −0.1±0.5 | 1.0±0.4 | 1.0±0.4 | −0.2±0.5 | 0.0±0.6 |
| HMW adiponectin (mg/L) | 40±2 | 39±3 | 20±3 | 21±2 | −20±3 | −18±3 | 14±2 | 13±1 | −26±3 | −26±4 |
| IGF-I (nmol/L) | 70±10 | 34±2‡ | 62±7 | 66±7 | −8±13 | 32±7‡ | 82±9 | 86±10 | 12±9 | **52±10*** |
| TG (mmol/L) | – | – | 1.2±0.2 | 1.2±0.1 | – | – | 0.9±0.1 | 0.8±0.1 | – | – |
| HDL-C (mmol/L) | – | – | 0.9±0.1 | 1.1±0.1* | – | – | 1.2±0.1 | 1.1±0.1 | – | – |
| LDL-C (mmol/L) | – | – | 2.3±0.1 | 2.2±0.2 | – | – | 2.6±0.1 | 2.6±0.2 | – | – |
| Body composition (DXA) | | | | | | | | | | |
| Age at DXA (days) | 14±1 | 13±1 | 374±6 | 389±11 | 360±6 | 375±11 | 760±10 | 759±14 | 746±11 | 746±14 |
| Fat mass (kg) | 0.7±0.1 | 0.5±0.1† | 3.6±0.1 | 3.0±0.1‡ | 2.9±0.1 | 2.6±0.1 | 3.9±0.2 | **3.2±0.2*** | 3.2±0.2 | 2.8±0.2 |
| Abdominal fat (kg) | 0.03±0.00 | 0.02±0.00† | 0.19±0.01 | 0.17±0.02 | 0.16±0.01 | 0.15±0.02 | 0.18±0.02 | 0.14±0.01 | 0.16±0.02 | 0.13±0.01 |
| Lean mass (kg) | 3.1±0.1 | 2.3±0.1† | 6.9±0.1 | 5.9±0.1 | 3.8±0.1 | 3.7±0.1 | 8.5±0.2 | 8.0±0.2 | 5.9±0.2 | 5.3±0.2 |

Data are mean±SEM. *p<0.05, ‡p<0.01 and †p<0.001 between subgroups.
The assessments at 24 months were performed in 26 AGA and 18 SGA infants. The bold values highlight the statistically significant differences.
BMI, body mass index; DXA, dual X-ray absorptiometry; HDL-C, HDL-cholesterol; HMW-adiponectin, high-molecular weight adiponectin; HOMA-IR, homeostatic model assessment-insulin resistance; IGF-I, insulin-like growth factor-I; LDL-C, LDL-cholesterol;TG, triglycerides.

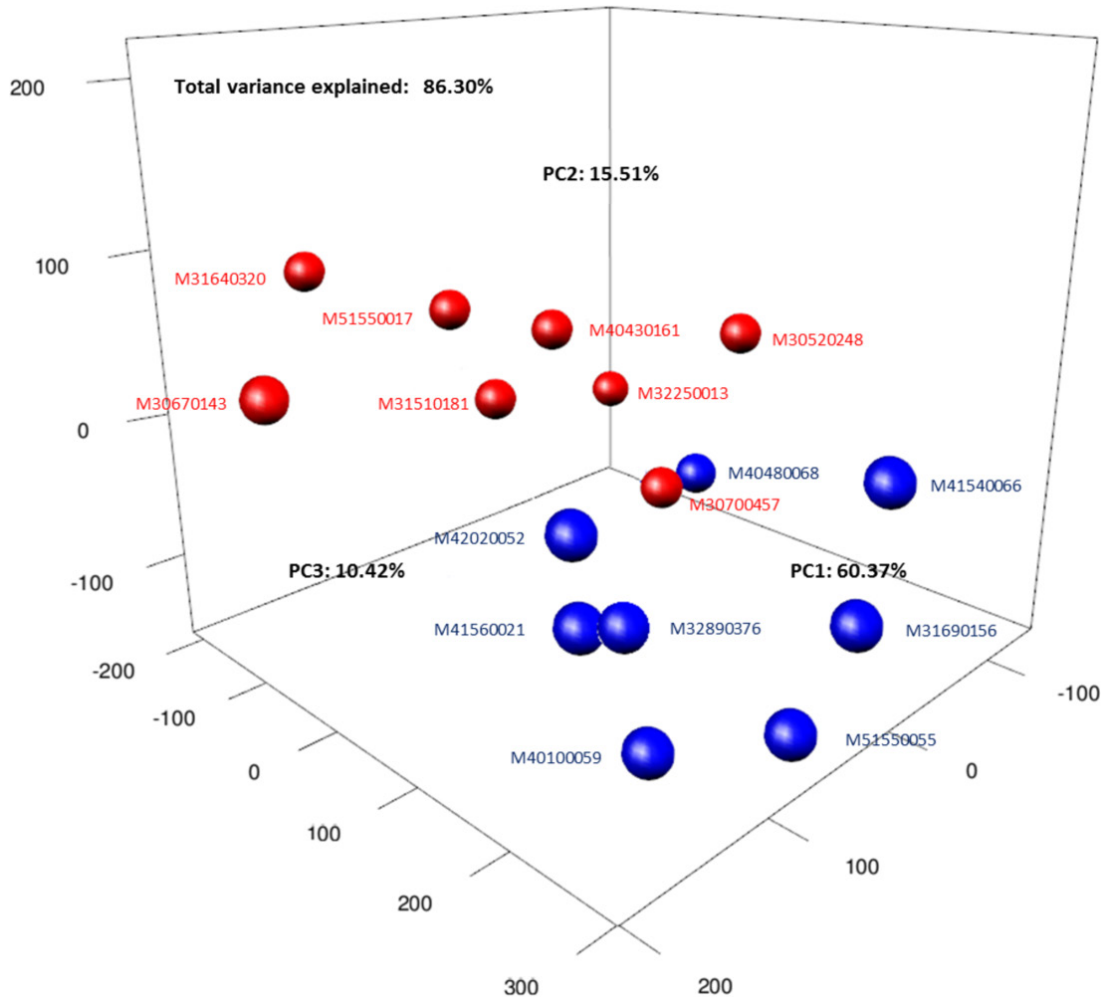


**Figure 1** Principal component analysis (PCA) of the methylation profiles from 8 AGA samples (red dots) and 8 SGA samples (blue dots). The PCA is based on $\log_2$ ratios and the methylation profiles are across all the 27,800 CpG sites in the microarray. The first three principal components are plotted. The captured variances of PC1 (first principal component), PC2 (second principal component) and PC3 (third principal component) were 60.4%, 15.5% and 10.4%, respectively. AGA, appropiate-for-gestational-age; SGA, small-for-gestational-age.

Circulating levels of LDL-C were associated with the methylation pattern of *FABP5*, *GAS6* and *CPT1A* genes at age 24 months.

### Multivariate linear models

In linear regression analysis adjusted for sex and BMI Z-score, methylation status of *NKX6.1* and *GPR120* were independent predictors of total fat at age 12 months and 24 months, respectively (online supplemental table 6). Lean mass was independently explained by *SLC2A8* methylation at the age of 12 months and by *ONECUT1* methylation at 24 months (online supplemental table 6). Moreover, *SLC2A8* methylation independently explained 42% of the 0–24 month changes in BMI Z-score variability (online supplemental table 6).

## DISCUSSION

Here, we report for the first time a differential DNA methylation profile in peripheral blood of SGA infants aged 12 months, its association with BMI, body composition parameters and markers of insulin resistance at 12 and at 24 months, and its potential contribution to an altered fat distribution on postnatal catch-up in weight. We identified n=41 differentially methylated CpG sites in gene promotor regions; 13 CpG were hypermethylated and located in *GPR120*, *NKX6.1*, *CPT1A*, *IGFBP4* genes and 28 CpG were hypomethylated along the *CHGA*, *FABP5*, *CTRP1*, *GAS6*, *ONECUT1* and *SLC2A8* genes.

*GPR120* is a functional receptor for n–3 fatty acids and a key regulator of adipogenesis, as well as of energy metabolism, insulin secretion and inflammation.[20–22] *GPR120* deficiency leads to obesity, insulin resistance and hepatic steatosis in mice fed a high-fat diet.[23] In contrast, activation of *GPR120* increases insulin secretion, protects pancreatic β cells from inflammation,[24] and reduces fat mass and body weight through activation of brown adipose tissue (BAT) thermogenesis[25]; *GPR120* is also required for neonatal adaptive thermogenesis in mice.[26] We have previously reported that *GPR120* is hypermethylated in cord blood of SGA infants and that it associates with birth weight and reduced fat mass across

**Table 2** Gene Ontology (GO) analysis of differentially methylated genes (n=129)

| | Observed genes | P value |
|---|---|---|
| (a) Biological processes | | |
| Regulation of metabolic processes | 39 | 8.30E−05 |
| Glucose metabolism | 4 | 4.70E−05 |
| Lipid metabolism | 4 | 3.40E−05 |
| Organ development | 24 | 7.70E−04 |
| Cellular signaling | 3 | 4.50E−04 |
| Regulation of immunity | 3 | 1.30E−04 |
| Cell adhesion | 5 | 2.40E−03 |
| Cell differentiation | 2 | 1.70E−03 |
| (b) Molecular functions | | |
| Transcription regulation | 23 | 3.70E−04 |
| DNA binding | 32 | 6.30E−03 |
| (c) Cellular components | | |
| Integral to membrane organization | 10 | 1.80E−03 |
| Intrinsic to plasma membrane | 7 | 1.50E−03 |

(a) Biological Processes, (b) Molecular function and (c) Cellular components.
Significant enriched components are grouped according to three categories.

early infancy, suggesting that *GPR120* could be among the mediators of early fat mass accretion via modulating adipogenesis and lipogenesis.[13] Here, we show that this methylation pattern is maintained in late infancy, and associates with lower BMI Z-scores and less fat mass, and with higher HOMA-IR. *IGFBP4*, which controls adipose tissue expansion by suppressing IGF-I signaling and angiogenesis promotion,[27] was also hypermethylated in SGA infants. Overall, the combined abnormal methylation of *GPR120* and *IGFBP4* and ensuing deregulation could result in an impaired adipogenesis in SGA infants.

*NKX6.1* is a transcription factor playing a key role in prenatal β-cell differentiation and in postnatal β-cell proliferation and function.[28] This gene was found to be hypermethylated and downregulated in SGA infants at birth,[13] and here we show that this pattern is still detectable at age 12 months. Cells lacking *NKX6.1* are unable to express PDX1 and MAFA, both transcription factors needed for the maintenance of β-cell identity and function.[29] Interestingly, a recent report showed that *GPR120* prevents lipid-induced β-cell damage through regulation of PDX1 expression. Moreover, *ONECUT1*—a hepatocyte nuclear factor with a programmed downregulation during pancreas development—acts as MAFA suppressor, and the inappropriate reactivation of this transcriptional regulator occurs in diabetes.[30 31] It is thus tempting to speculate that the abnormal methylation of *GRP120* and *NKX6.1* in SGA infants, already detectable at birth and ongoing at age 12 months, together with the hypomethylation of *ONECUT1*, may negatively affect β-cell number, as suggested by the association between the methylation status of these genes and HOMA-IR, fat mass and BMI Z-scores. At age 24 months, SGA infants still have normal levels of IGF-I and HMW adiponectin, less fat mass and are insulin sensitive; however, by age 3 years, SGA children develop high IGF-I levels, a thicker carotida and lower concentrations of HMW adiponectin,[32] supporting the notion that the impairment of insulin action may occur from age 2 years onwards. This phenotype aligns well with the abnormal methylation by age 12 months of several genes related to the control of glucose and lipid metabolism. For example, *FABP5*, which is involved in the regulation of adipose tissue function and inflammation[33 34] was hypomethylated in SGA infants, and transgenic mice models have shown that *FABP5* overexpression impairs glucose tolerance, which is in turn reverted in *FABP5 knockout* mice[33]; *FABP5* also plays a role in the development of carotid atherosclerosis.[35] In addition, *CTRP1* was also hypomethylated in SGA infants, and is reported to increase in obesity, fatty liver disease, atherosclerosis and type 2 diabetes, and to be associated with major adverse cardiovascular events.[36 37]

At age 6 years, SGA infants are more insulin resistant and have more pre-peritoneal and hepatic fat than AGA infants.[32] Disruption of lipid homeostasis and reduced mitochondrial function are among the mechanisms that could contribute to this sequence of events. *CPT1A*, a key regulatory enzyme of β-oxidation required for transport of long-chain fatty acids into mitochondria, was hypermethylated in SGA infants. A decrease in fat oxidation may be followed by fat accumulation; for example, in rodents, the inhibition of fat oxidation results in an increase in intracellular lipids and a decrease in insulin action, whereas in humans an increased respiratory quotient (RQ), indicative of decreased fat oxidation, predicts weight gain and ectopic fat storage and is associated with a deterioration of insulin sensitivity.[38 39] Inversely, overexpression of *CPT1A* in the liver of obese mice reduces inflammation and improves insulin signaling.[40] Recently, epigenome-wide association studies have disclosed the causal role of *CPT1A* methylation in type 2 diabetes[41] and the association between intron 1 *CPT1A* methylation and gestational BMI.[42]

*SLC2A8*, also known as *GLUT8*, is a glucose and fructose transporter highly expressed in oxidative tissues and required for the development of fructose-induced hepatic steatosis.[43] *SLC2A8* hypomethylation could additionally contribute to the higher hepatic fat fraction in SGA infants since overexpression of *SLC2A8* in hepatocytes represses PPARγ and impairs fatty acid metabolism.[44]

*CHGA* is a prohormone secreted by neuroendocrine tissues serving as precursor of biologically active peptides including PST (pancreastatin) that interfere with insulin action. PST-treated adipocytes show a decrease in insulin-stimulated lipogenesis,[45] whereas *CHGA* null mice display increased insulin sensitivity,[46] even after a diet-induced

**Table 3** Differentially methylated genes involved in KEGG pathways

| Pathway | P value | Methylation status | Gene symbol |
|---|---|---|---|
| Lipid metabolism | 1.80E–05 | Hyper<br>Hypo | ***GPR120***, ***CPT1A***<br>***FABP5***, *LMF1*, ***CTRP1***, *TM6SF2, ELOVL5* |
| Cell development and function | 3.70E–05 | Hyper<br>Hypo | ***NKX6.1***, *SMAD7, GATAD2B, ADAMTS1, NR2F2, POU3F2, TTC30B, RUNX2, NPBWR1*<br>***IGFBP4***, *DNAI2, PDZRN3, AFTPH, EFNA5, NPAS3, KCNC3, MICAL2, SLC30A9, SLC22A15, NPAS3* |
| Glucose metabolism | 4.20E–05 | Hyper<br>Hypo | *RAB4B, **SIK2*<br>**TRAF2*, ***GAS6***, ***ONECUT1***, *MIDN*, ***SLC2A8***, *CTRP1, GPR4*, ***CHGA*** |
| Cellular signaling | 4.30E–04 | Hyper<br>Hypo | *ITPRIP, DUSP4, CHRM4, ATP2C1*<br>*PPP4R4, PCDHB2, ILK, SLC22A15, FGD5, CLSTN1, GNB1, DUSP7, INSRR, IL17RD, SLC2A8* |
| DNA binding | 5.10E–04 | Hyper<br>Hypo | *H2AFY, SMAD7, HIST1H2AJ, XRCC5*<br>*ZNF558, ETV3, ZNF141, ZNF7, EN2, ZZZ3, ZNF462, ZNF7* |
| Transcription regulation | 8.70E–04 | Hyper<br>Hypo | *HLX, BCL6, PATZ1, POU3F2, FOXB1, NR2F2, RUNX2, C1orf113, POU4F1, C7orf64, DDX17*<br>*JDP2, ETV7, ONECUT1, ZNF132, NPAS3, HBP1, EOMES, NEUROG2, ZFHX4, RNF4, HBP1, UTF1, SLC30A9, TAF4* |
| Regulation of immunity | 2.10E–03 | Hyper<br>Hypo | *TNFAIP8L1, LMBR1*<br>*ETV3, SUGT1, UBE2F, LONRF1* |
| Neural differentiation | 2.80E–03 | Hyper<br>Hypo | *POU3F2, FZD2, RUNX2*<br>*NEUROG2* |
| Regulation of apoptosis | 4.10E–03 | Hypo | TRAF2, ROBO4, PPP1R13B, GAS6 |
| Potassium channel | 8.80E–03 | Hyper<br>Hypo | *KCNC4*<br>*KCNC3, TMEM38A, CLIC6* |

Pathways are arranged (top to bottom) according to p value. The genes in bold (n=12) were selected for pyrosequencing validation in all the study subjects (n=30 AGA, n=21 SGA).
*Failed genes in pyrosequencing validation.
AGA, appropiate-for-gestational-age; KEGG, Kyoto Encyclopedia of Genes and Genomes; SGA, small-for-gestational-age.

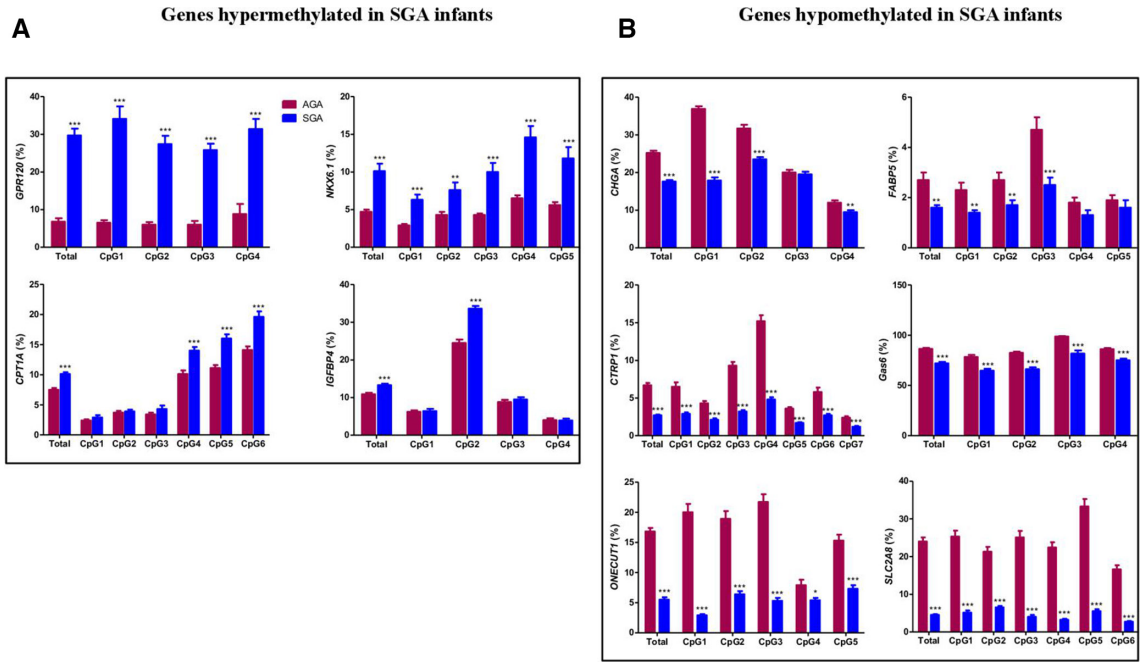


**Figure 2** Methylation levels of validated genes in peripheral blood from infants born appropriate-for-gestational-age (AGA, n=30) or small-for-gestational-age (SGA, n=21) at age 12 months. Left panel (A): *GPR120*, *NKX6.1*, *CPT1A* and *IGFBP4* were hypermethylated in SGA infants. Right panel (B): *CHGA, FABP5, CTRP1, GAS6, ONECUT1* and *SLC2A8* were hypomethylated in SGA infants. *p<0.05; **p<0.01; ***p<0.0001.

obesity, highlighting the importance of *CHGA*–PST interaction in the development of insulin resistance.[47] The hypomethylation of *CHGA* in SGA infants could hamper further subcutaneous adipogenesis favoring ectopic fat storage on catch-up in weight by inducing adipose tissue dysfunction.

The relevance of *GAS6* hypomethylation in SGA infants remains unclear since its role in cancer, obesity, inflammation and insulin resistance remains controversial.[48–50] *GAS6* is a member of the vitamin K–dependent protein family that binds to TAM (Tyro3, Axl and Mer) receptors; and high and low levels of *GAS6* have been reported, respectively, in overweight and obese adolescents,[49] and in patients with type 2 diabetes.[50]

The limitations of the present study include the relatively small size of the studied population, the absence of gene expression assessments, the lack of methylation analysis at age 24 months, the lack of adjustment for cell composition in peripheral blood and the absence of methylation/expression assessments in insulin-target tissues due to ethical restraints. The strengths include the strict inclusion criteria, the use of the same methods over time and the prospective design of the study, allowing to assess the associations of the methylation patterns with endocrine-metabolic and body composition markers over the first 2 years of life.

Overall, our results strengthen the notion that an adverse intrauterine environment can induce long-term changes in gene expression through epigenetic mechanisms, which in turn can predispose to metabolic disorders.

In conclusion, we identified altered epigenetic marks in peripheral blood of SGA infants in genes involved in the control of adipogenesis and energy homeostasis that may exert long-term programming effects and thus increase the risk for obesity and diabetes in this population.

**Author affiliations**
[1]Endocrinology Department, Institut Pediàtric Hospital Sant Joan de Déu, University of Barcelona, Esplugues, Barcelona, Spain
[2]Centro de Investigación Biomédica en Red de Diabetes y Enfermedades Metabólicas Asociadas (CIBERDEM), ISCIII, Madrid, Spain
[3]Department of Pediatrics, Dr. Josep Trueta Hospital and Girona Institute for Biomedical Research, Girona, Spain
[4]Department of Development & Regeneration, University of Leuven, Leuven, Flanders, Belgium

**Contributors** MD contributed to study design, researched data, wrote the manuscript and reviewed/edited manuscript. EG researched data. AL-B and FdZ reviewed/edited the manuscript. LI contributed to study design, wrote the manuscript and reviewed/edited the manuscript. LI and MD are Clinical Investigators of CIBERDEM (Centro de Investigación Biomédica en Red de Diabetes y Enfermedades Metabólicas Asociadas, Instituto de Salud Carlos III, Madrid, Spain). AL-B is a Clinical Investigator of the I3 Fund for Scientific Research (Ministry of Science and Innovation, Spain). LI is the guarantor of this work and, as such, had full access to all the data in the study and takes responsibility for the integrity of the data and the accuracy of the data analysis.

**Funding** This study was supported by the Ministerio de Ciencia e Innovación, Instituto de Salud Carlos III, and by the Fondo Europeo de Desarrollo Regional (FEDER) (PI11/02403).

**Competing interests** None declared.

**Patient consent for publication** Not required.

**Ethics approval** The study was approved by the Institutional Review Board of Hospital Sant Joan de Déu at Barcelona University (PIC-51-11).

**Provenance and peer review** Not commissioned; externally peer reviewed.

**Data availability statement** Data are available on reasonable request. The datasets generated during and/or analyzed during the current study are available from the corresponding author on reasonable request.



**ORCID iD**
Lourdes Ibañez http://orcid.org/0000-0003-4595-7191

## REFERENCES

1 Leunissen RWJ, Kerkhof GF, Stijnen T, *et al*. Timing and tempo of first-year rapid growth in relation to cardiovascular and metabolic risk profile in early adulthood. *JAMA* 2009;301:2234–42.
2 Nakano Y. Adult-onset diseases in low birth weight infants: association with adipose tissue maldevelopment. *J Atheroscler Thromb* 2020;27:397–405.
3 Gluckman PD, Hanson MA, Beedle AS, *et al*. Predictive adaptive responses in perspective. *Trends Endocrinol Metab* 2008;19:109–10.
4 de Zegher F, Malpique R, Garcia-Beltran C, *et al*. Towards a simple marker of hepato-visceral adiposity and insulin resistance: the Z-score change from weight-at-birth to BMI-in-childhood. *Pediatr Obes* 2019;14:e12533.
5 de Zegher F, Sebastiani G, Diaz M, *et al*. Breast-feeding vs formula-feeding for infants born small-for-gestational-age: divergent effects on fat mass and on circulating IGF-I and high-molecular-weight adiponectin in late infancy. *J Clin Endocrinol Metab* 2013;98:1242–7.
6 Park JH, Stoffers DA, Nicholls RD, *et al*. Development of type 2 diabetes following intrauterine growth retardation in rats is associated with progressive epigenetic silencing of Pdx1. *J Clin Invest* 2008;118:2316–24.
7 Einstein F, Thompson RF, Bhagat TD, *et al*. Cytosine methylation dysregulation in neonates following intrauterine growth restriction. *PLoS One* 2010;5:e8887.
8 Rodríguez-Rodríguez P, Ramiro-Cortijo D, Reyes-Hernández CG, *et al*. Implication of oxidative stress in fetal programming of cardiovascular disease. *Front Physiol* 2018;9:602.
9 Blondeau B, Avril I, Duchene B, *et al*. Endocrine pancreas development is altered in foetuses from rats previously showing intra-uterine growth retardation in response to malnutrition. *Diabetologia* 2002;45:394–401.
10 Tobi EW, Lumey LH, Talens RP, *et al*. DNA methylation differences after exposure to prenatal famine are common and timing- and sex-specific. *Hum Mol Genet* 2009;18:4046–53.
11 Lukaszewski M-A, Eberlé D, Vieau D, *et al*. Nutritional manipulations in the perinatal period program adipose tissue in offspring. *Am J Physiol Endocrinol Metab* 2013;305:E1195–207.
12 García-Carpizo V, Ruiz-Llorente L, Fraga M, *et al*. The growing role of gene methylation on endocrine function. *J Mol Endocrinol* 2011;47:R75–89.
13 Díaz M, García C, Sebastiani G, *et al*. Placental and cord blood methylation of genes involved in energy homeostasis: association with fetal growth and neonatal body composition. *Diabetes* 2017;66:779–84.
14 Simpkin AJ, Suderman M, Gaunt TR, *et al*. Longitudinal analysis of DNA methylation associated with birth weight and gestational age. *Hum Mol Genet* 2015;24:3752–63.

15 Alisch RS, Barwick BG, Chopra P, *et al*. Age-associated DNA methylation in pediatric populations. *Genome Res* 2012;22:623–32.
16 Wang D, Liu X, Zhou Y, *et al*. Individual variation and longitudinal pattern of genome-wide DNA methylation from birth to the first two years of life. *Epigenetics* 2012;7:594–605.
17 Martino D, Loke YJ, Gordon L, *et al*. Longitudinal, genome-scale analysis of DNA methylation in twins from birth to 18 months of age reveals rapid epigenetic change in early life and pair-specific effects of discordance. *Genome Biol* 2013;14:R42.
18 Clayton PE, Cianfarani S, Czernichow P, *et al*. Management of the child born small for gestational age through to adulthood: a consensus statement of the International Societies of Pediatric Endocrinology and the Growth Hormone Research Society. *J Clin Endocrinol Metab* 2007;92:804–10.
19 Ferrández-Longas A, Mayayo E, Labarta JI, *et al*. Estudio longitudinal de crecimiento y desarrollo. Centro Andrea Prader. Zaragoza 1980–2002. In: Garcia-Dihinx A, Romo A, Ferrandez-Longas A, *et al*, eds. *Patrones de crecimiento y desarrollo en España. Ergon*. Madrid, Spain, 2004: 61–115.
20 Hilgendorf KI, Johnson CT, Mezger A, *et al*. Omega-3 fatty acids activate ciliary FFAR4 to control adipogenesis. *Cell* 2019;179:1289–305.
21 Amos D, Cook C, Santanam N. Omega 3 rich diet modulates energy metabolism via GPR120-Nrf2 crosstalk in a novel antioxidant mouse model. *Biochim Biophys Acta Mol Cell Biol Lipids* 2019;1864:466–88.
22 Zhao YY, Fu H, Liang XY, *et al*. Lipopolysaccharide inhibits GPR120 expression in macrophages via Toll-like receptor 4 and p38 MAPK activation. *Cell Biol Int*.
23 Ichimura A, Hirasawa A, Poulain-Godefroy O, *et al*. Dysfunction of lipid sensor GPR120 leads to obesity in both mouse and human. *Nature* 2012;483:350–4.
24 Schilperoort M, van Dam AD, Hoeke G, *et al*. The GPR120 agonist TUG-891 promotes metabolic health by stimulating mitochondrial respiration in brown fat. *EMBO Mol Med* 2018;10:pii:e8047.
25 Quesada-López T, Gavaldà-Navarro A, Morón-Ros S, *et al*. Gpr120 controls neonatal brown adipose tissue thermogenic induction. *Am J Physiol Endocrinol Metab* 2019;317:E742–50.
26 Wang Y, Xie T, Zhang D, *et al*. GPR120 protects lipotoxicity-induced pancreatic β-cell dysfunction through regulation of PDX1 expression and inhibition of islet inflammation. *Clin Sci* 2019;133:101–16.
27 Gealekman O, Gurav K, Chouinard M, *et al*. Control of adipose tissue expandability in response to high fat diet by the insulin-like growth factor-binding protein-4. *J Biol Chem* 2014;289:18327–38.
28 Taylor BL, Benthuysen J, Sander M. Postnatal β-cell proliferation and mass expansion is dependent on the transcription factor Nkx6.1. *Diabetes* 2015;64:897–903.
29 Schaffer AE, Taylor BL, Benthuysen JR, *et al*. Nkx6.1 controls a gene regulatory network required for establishing and maintaining pancreatic beta cell identity. *PLoS Genet* 2013;9:e1003274.
30 Tweedie E, Artner I, Crawford L, *et al*. Maintenance of hepatic nuclear factor 6 in postnatal islets impairs terminal differentiation and function of beta-cells. *Diabetes* 2006;55:3264–70.
31 Yamamoto K, Matsuoka T-aki, Kawashima S, *et al*. A novel function of Onecut1 protein as a negative regulator of MafA gene expression. *J Biol Chem* 2013;288:21648–58.
32 Sebastiani G, Díaz M, Bassols J, *et al*. The sequence of prenatal growth restraint and post-natal catch-up growth leads to a thicker intima–media and more pre-peritoneal and hepatic fat by age 3–6 years. *Pediatr Obes* 2016;11:251–7.
33 Maeda K, Uysal KT, Makowski L, *et al*. Role of the fatty acid binding protein MAL1 in obesity and insulin resistance. *Diabetes* 2003;52:300–7.
34 Shibue K, Yamane S, Harada N, *et al*. Fatty acid-binding protein 5 regulates diet-induced obesity via GIP secretion from enteroendocrine K cells in response to fat ingestion. *Am J Physiol Endocrinol Metab* 2015;308:E583–91.
35 Furuhashi M, Ogura M, Matsumoto M, *et al*. Serum FABP5 concentration is a potential biomarker for residual risk of atherosclerosis in relation to cholesterol efflux from macrophages. *Sci Rep* 2017;7:217.
36 Shabani P, Naeimi Khaledi H, Beigy M, *et al*. Circulating level of CTRP1 in patients with nonalcoholic fatty liver disease (NAFLD): is it through insulin resistance? *PLoS One* 2015;10:e0118650.
37 Muendlein A, Leiherer A, Saely C, *et al*. The novel adipokine CTRP1 is significantly associated with the incidence of major adverse cardiovascular events. *Atherosclerosis* 2019;286:1–6.
38 Dobbins RL, Szczepaniak LS, Bentley B, *et al*. Prolonged inhibition of muscle carnitine palmitoyltransferase-1 promotes intramyocellular lipid accumulation and insulin resistance in rats. *Diabetes* 2001;50:123–30.
39 Zurlo F, Lillioja S, Esposito-Del Puente A, *et al*. Low ratio of fat to carbohydrate oxidation as predictor of weight gain: study of 24-h RQ. *Am J Physiol* 1990;259:E650–7.
40 Orellana-Gavaldà JM, Herrero L, Malandrino MI, *et al*. Molecular therapy for obesity and diabetes based on a long-term increase in hepatic fatty-acid oxidation. *Hepatology* 2011;53:821–32.
41 Cardona A, Day FR, Perry JRB, *et al*. Epigenome-wide association study of incident type 2 diabetes in a British population: EPIC-Norfolk study. *Diabetes* 2019;68:2315–26.
42 Pavethynath S, Imai C, Jin X, *et al*. Metabolic and immunological shifts during mid-to-late gestation influence maternal blood methylation of *CPT1A* and *SREBF1*. *Int J Mol Sci* 2019;20:1066.
43 Debosch BJ, Chen Z, Saben JL, *et al*. Glucose transporter 8 (GLUT8) mediates fructose-induced de novo lipogenesis and macrosteatosis. *J Biol Chem* 2014;289:10989–98.
44 DeBosch BJ, Chen Z, Finck BN, *et al*. Glucose transporter-8 (GLUT8) mediates glucose intolerance and dyslipidemia in high-fructose diet-fed male mice. *Mol Endocrinol* 2013;27:1887–96.
45 Sánchez-Margalet V, González-Yanes C. Pancreastatin inhibits insulin action in rat adipocytes. *Am J Physiol* 1998;275:E1055–60.
46 Gayen JR, Saberi M, Schenk S, *et al*. A novel pathway of insulin sensitivity in chromogranin A null mice: a crucial role for pancreastatin in glucose homeostasis. *J Biol Chem* 2009;284:28498–509.
47 Bandyopadhyay GK, Lu M, Avolio E, *et al*. Pancreastatin-dependent inflammatory signaling mediates obesity-induced insulin resistance. *Diabetes* 2015;64:104–16.
48 Wu K-S, Hung Y-J, Lee C-H, *et al*. The involvement of GAS6 signaling in the development of obesity and associated inflammation. *Int J Endocrinol* 2015;2015:202513.
49 Hsiao F-C, Lin Y-F, Hsieh P-S, *et al*. Circulating growth arrest-specific 6 protein is associated with adiposity, systemic inflammation, and insulin resistance among overweight and obese adolescents. *J Clin Endocrinol Metab* 2013;98:E267–74.
50 Hung Y-J, Lee C-H, Chu N-F, *et al*. Plasma protein growth arrest-specific 6 levels are associated with altered glucose tolerance, inflammation, and endothelial dysfunction. *Diabetes Care* 2010;33:1840–4.